Dinuclear and Trinuclear Ni−, Pd−, and Pt−Halide Complexes of the Easily Accessible Chiral Ligand *P*,*P*,*P′*-Tris[(+)-9-phenyldeltacyclan-8-yl]-1,2-bis(phosphanyl)benzene[‡]

Henri Brunner,*[a] Stephan Dormeier,[a] Ilias Grau,[a] and Manfred Zabel[a]

Dedicated to Professor Dr. Gottfried Huttner on the occasion of his 65th birthday

Keywords: Nickel complexes / Palladium complexes / Platinum complexes / Phosphido bridges / Phosphorus configuration

The synthesis of seven dinuclear complexes **[(+)$_\delta$-LMHal]$_2$** (M = Ni, Pd, Pt; Hal = Cl, Br, I) is described, in which **(+)$_\delta$-L$^-$** represents the deprotonated chiral chelate ligand *P,P,P′*-tris[(+)-9-phenyldeltacyclan-8-yl]-1,2-bis(phosphanyl)-benzene, easily accessible in a highly enantioselective homo-Diels–Alder reaction. All the dinuclear complexes are bent at the phosphido bridges which connect the two square-planar halves of the molecules. The phosphorus atoms of the phosphido bridges are stereogenic centers. For **[(+)$_\delta$-LNiBr]$_2$** and **[(+)$_\delta$-LPdCl]$_2$** both diastereomers with (S_P,S_P) and (R_P,R_P) configuration were observed, whereas for **[(+)$_\delta$-LPdBr]$_2$**, **[(+)$_\delta$-LPdI]$_2$**, and **[(+)$_\delta$-LPtCl]$_2$** only the (S_P,S_P) isomers could be obtained. Furthermore, the synthesis of eight trinuclear complexes **[(+)$_\delta$-L$_2$M$_3$Hal$_4$]** (M = Pd, Pt; Hal = Cl, Br) is reported, which contain unusual three-square arrays. In the trinuclear complexes all the halogens are oriented to one side. Halogeno and phosphido bridges connect the three squares leading to chair configurations (opposite scaffold chirality possible) and boat configurations. For **[(+)$_\delta$-L$_2$Pd$_3$Cl$_4$]**, **[(+)$_\delta$-L$_2$Pd$_3$Br$_4$]**, and **[(+)$_\delta$-L$_2$Pt$_3$Cl$_4$]** the two diastereomers with (S_P,S_P) and (R_P,R_P) configuration and for **[(+)$_\delta$-L$_2$Pt$_3$Br$_4$]** the diastereomers with (S_P,S_P) and (S_P,R_P) configuration could be isolated. In addition, the dinuclear complex **[(+)$_\delta$-LPt$_2$Br$_3$(cod)]** (cod = 1,5-cyclooctadiene) containing a single phosphido bridge was obtained.

Introduction

In the previous paper the synthesis of the chiral ligand *P*,*P*,*P′*-tris[(+)-9-phenyldeltacyclan-8-yl)-1,2-bis(phosphanyl)benzene **(+)$_\delta$-LH** and its mononuclear complexes was reported. **(+)$_\delta$-LH** is formed in the enantioselective homo-Diels−Alder reaction of norbornadiene with phenylacetylene[2,3] and the subsequent addition of 3 PH bonds of 1,2-bis(phosphanyl)benzene to the double bonds of (+)-8-phenyldeltacyclene.[1,4] **(+)$_\delta$-LH** contains 3 × 8 = 24 asymmetric carbon atoms in its three deltacyclanyl substituents and a stereogenic secondary phosphorus atom which is configurationally labile in the free ligand but stabilized in its mononuclear complexes **[(+)$_\delta$-LH]MHal$_2$**, M = Ni, Pd, Pt.[1] The symbol **(+)$_\delta$** in the ligand **(+)$_\delta$-LH** and in its complexes indicates the 24 asymmetric carbon atoms of a given configuration in the deltacyclane substituents built up in the highly enantioselective homo-Diels−Alder reaction. Here, the dinuclear and trinuclear compounds will be described, which form on HHal elimination from the complexes **[(+)$_\delta$-LH]MHal$_2$**.[5] The dinuclear complexes have roof-shaped structures with bridging phosphorus atoms. In the trinuclear compounds three square-planar units are connected in an uncommon way. In addition to the 48 asymmetric carbon atoms of fixed configuration both dinuclear and trinuclear complexes contain two stereogenic phosphorus atoms of the phosphido bridges. As the phosphorus atoms may occur in (S_P,S_P) as well as (R_P,R_P) in one case even (S_P,R_P) configuration series of diastereomers could be isolated and characterized differing only in the configuration of the phosphido bridges. Thus, the dinuclear compounds **(S_P,S_P)-** and **(R_P,R_P)-[(+)$_\delta$-MHal]$_2$** and the trinuclear compounds **(S_P,S_P)-**, **(R_P,R_P)-** and **(S_P,R_P)-[(+)$_\delta$-L$_2$M$_3$Hal$_4$]** are not enantiomers but diastereomers.

All the molecules shown in Schemes 1 and 2 and discussed in Tables 1−6 {except **(R_P)-[(+)$_\delta$-L$_2$Pt$_3$Br$_3$(cod)]**} are C_2-symmetric. However, only for **(S_P,S_P)-[(+)$_\delta$-L$_2$Pd$_3$Br$_4$]**, **(R_P,R_P)-[(+)$_\delta$-L$_2$Pd$_3$Br$_4$]**, and **(S_P,S_P)-[(+)$_\delta$-L$_2$Pt$_3$Br$_4$]** the C_2 axis of the molecule is also a symmetry element of the unit cell. Consequently, in all the other cases the two halves of the molecules are different. Nevertheless, throughout the paper only one half of each molecule is described and discussed (the left halves in Figures 1−5).

[‡] Enantioselective Catalysis, 145. Part 144: Ref.[1]

[a] Institut für Anorganische Chemie, Universität Regensburg,
93040 Regensburg, Germany
Fax: (internat.) + 49-941/943-4439
E-mail: henri.brunner@chemie.uni-regensburg.de

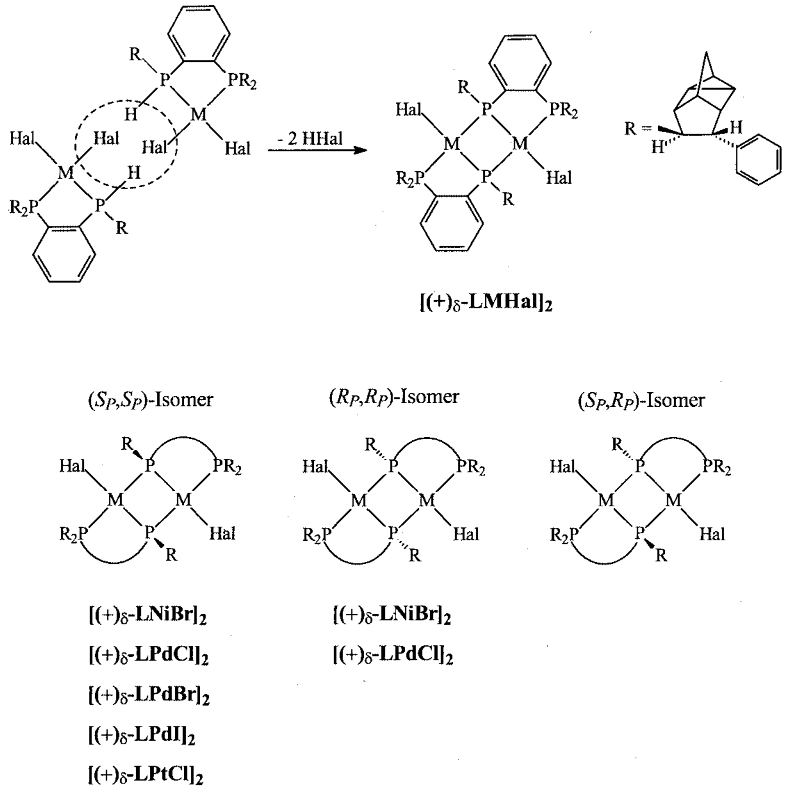

Scheme 1. Reaction of two mononuclear complexes **[(+)$_δ$-LH]MHal$_2$** to give the dinuclear phosphido-bridged compounds **[(+)$_δ$-LMHal]$_2$** (top) and the three possible isomers **(S_P,S_P)**-, **(R_P,R_P)**-, and **(S_P,R_P)-[(+)$_δ$-LMHal]$_2$** (bottom)

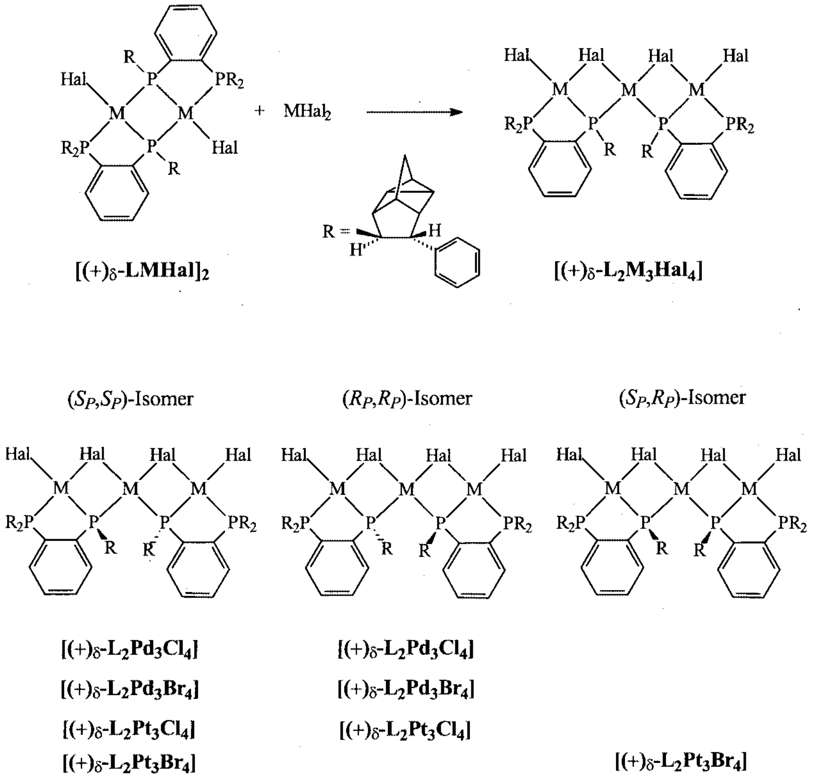

Scheme 2. Reaction of a dinuclear complex **[(+)$_δ$-LMHal]$_2$** and MHal$_2$ to give trinuclear compounds **[(+)$_δ$-L$_2$M$_3$Hal$_4$]** (top) and the three possible isomers **(S_P,S_P)**-, **(R_P,R_P)**-, and **(S_P,R_P)-[(+)$_δ$-L$_2$M$_3$Hal$_4$]** of the trinuclear phosphido- and halo-bridged complexes having all the halides on one side (bottom)

The Dinuclear Phosphido-Bridged Complexes [(+)$_{\delta}$-LMHal]$_{2}$

Although most of the syntheses of the dinuclear complexes **[(+)$_{\delta}$-LMHal]$_{2}$** given in the Exp. Sect. started from the ligand **(+)$_{\delta}$-LH** and suitable metal precursors, the intermediacy of the corresponding mononuclear complexes **[(+)$_{\delta}$-LH]MHal$_{2}$** must be assumed.[1] As indicated in Scheme 1 two mononuclear complexes give the dinuclear phosphido-bridged compounds by twofold HHal elimination. Some of the dinuclear complexes were obtained in attempts to recrystallize the mononuclear compounds **[(+)$_{\delta}$-LH]MHal$_{2}$** demonstrating their tendency to loose HHal.

In the dinuclear complexes **[(+)$_{\delta}$-LMHal]$_{2}$** two square-planar units are connected by bridging phosphorus atoms. The phosphorus atoms of these phosphido bridges are stereogenic centers, as they have four different substituents: the palladium atom which is part of the chelate ring, the palladium atom which is not part of the chelate ring, the chelate ring, and the (+)-9-phenyldeltacyclanyl substituent. This priority sequence is the basis for the assignment of (*R*) and (*S*) configuration to these stereogenic phosphido phosphorus atoms. In all the dinuclear complexes **[(+)$_{\delta}$-LMHal]$_{2}$** the (+)-9-phenyldeltacyclanyl substituents have the same stereochemistry. It is the configuration of the bridging phosphorus atoms which differentiates the diastereomers.

At the bottom of Scheme 1 the three possible isomers for the dinuclear complexes are shown. In combination with the enantiomerically pure deltacyclane substituents abbreviated by **(+)$_{\delta}$** the configuration of the bridging phosphorus atoms can be (S_P,S_P), (R_P,R_P), or (S_P,R_P) giving rise to three diastereomers. Obviously, the **(S_P,S_P)-[(+)$_{\delta}$-LMHal]$_{2}$** diastereomers are highly favored. However, for the fragments NiBr and PdCl both diastereomers **(S_P,S_P)-** and **(R_P,R_P)-[(+)$_{\delta}$-LMHal]$_{2}$** could be isolated and characterized. The **(S_P,R_P)-[(+)$_{\delta}$-LMHal]$_{2}$** isomer, *meso*-configurated with respect to the central core (excluding the deltacyclanyl substituents), was never observed.

Dinuclear complexes in which two square-planar units are connected by bridges can be coplanar or bent.[6,7] Diphenylphosphido-bridged complexes usually are planar, e.g. [Hal(PPh$_2$H)M(μ-PPh$_2$)$_2$M(PPh$_2$H)Hal] (M = Pd, Pt; Hal = Cl, I).[8−10] On the other hand complexes containing unsymmetrically substituted phosphido bridges PRR′ are bent.[6] Consequently, the bridging phosphido groups discussed here, in which the phosphorus atoms have a phenylene and a deltacyclanyl substituent, are expected to be bent, the roof angle depending on the type of diastereomer.

Reaction of anhydrous NiBr$_2$ with **(+)$_{\delta}$-HL** and Na$_2$CO$_3$ in boiling ethanol provided a crude product, the ^{31}P NMR spectrum of which showed the signals of several compounds including those of the dinuclear complexes **(S_P,S_P)-[(+)$_{\delta}$-LNiBr]$_{2}$** (main product) and **(R_P,R_P)-[(+)$_{\delta}$-LNiBr]$_{2}$** (see below). Crystallization from CH$_2$Cl$_2$ gave red needles suitable for X-ray structure analysis. The ^{31}P NMR spectrum exhibited the AA′XX′ system of only one of the possible diastereomers. The structural study confirmed the dinuclear character of the complex (Figure 1) proving the presence of only one of the possible isomers.

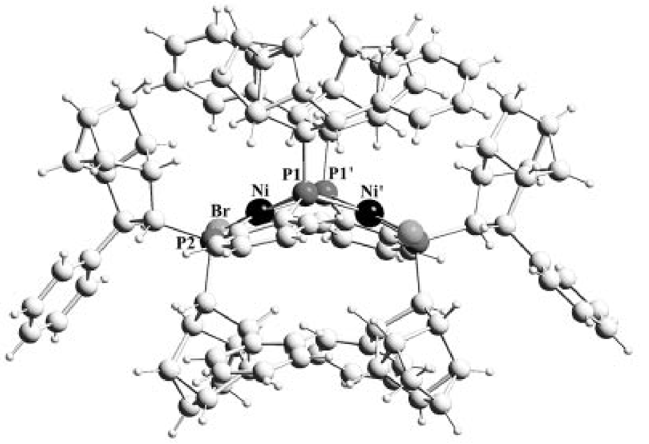

Figure 1. Molecular structure of **(S_P,S_P)-[(+)$_{\delta}$-LNiBr]$_{2}$**, crystallized from CH$_2$Cl$_2$; selected bond lengths [Å], bond angles [°], and dihedral angles [°]: Ni···Ni′ = 3.277(12), P1···P1′ = 2.689(8), Ni−Br = 2.349(1), Ni−P1 = 2.181(3), Ni−P1′ = 2.217(1), Ni−P2 = 2.207(3); Br−Ni−P1′ = 97.60(3), P1′−Ni−P1 = 75.39(4), P1−Ni−P2 = 88.39(4), P2−Ni−Br = 98.30(3), P1−Ni−Br = 172.95(3), P1′−Ni−P2 = 160.29(4); Ni−P1′−P1−Br = 0.53(2), Ni−P1′−P1−P2 = 8.24(3), P2−P1−P1′−Br = 7.71(3), Ni−P1−P1′−Ni′ = 140.84(4), Ni−P1−P2/C1−C2 = 10.5(2): δ

The configuration of the two bridging chiral phosphorus atoms was determined as (**S_P,S_P**). **(S_P,S_P)-[(+)$_{\delta}$-LNiBr]$_{2}$** is bent at the phosphido bridges. The "roof angle" between the two square-planar units is 140.84°. The dihedral angle of the metal substituents P2−P1−P1′−Br (of the left half of the molecule) shows that there is a small deformation of the square-planar arrangement of 7.71°. The chelate ring Ni−P1−C1−C2−P2 is slightly puckered indicated by the inclination of the bond C1−C2 of the benzene ring with respect to the plane Ni−P1−P2. The angle of this inclination is a measure of the chirality of the helix defined by the two skew lines C1−C2 and P1−P2 (which is part of the plane Ni−P1−P2). The chirality of the chelate ring Ni−P1−C1−C2−P2 is induced by the given chirality of the deltacyclanyl substituents and the configuration of the bridging phosphorus atoms. In **(S_P,S_P)-[(+)$_{\delta}$-LNiBr]$_{2}$** the inclination angle of C1−C2 with respect to the plane Ni−P1−P2 is 10.5°, defining δ helicity. The parameters discussed for **(S_P,S_P)-[(+)$_{\delta}$-LNiBr]$_{2}$** are typical for the (S_P,S_P) diastereomers. They differ for the (R_P,R_P) diastereomers (Table 1).

Reaction of anhydrous NiBr$_2$ with **(+)$_{\delta}$-HL** and *n*BuLi in CH$_2$Cl$_2$, followed by crystallization from acetone, afforded brown crystals of **(R_P,R_P)-[(+)$_{\delta}$-LNiBr]$_{2}$** suitable for X-ray structure analysis (Figure 2).

The diastereomer **(R_P,R_P)-[(+)$_{\delta}$-LNiBr]$_{2}$** is also bent at the phosphido bridges. However, the roof angle of 156.53° shows a flattening compared to **(S_P,S_P)-[(+)$_{\delta}$-LNiBr]$_{2}$**, which is also obvious from the lengthening of the nonbonding Ni−Ni distance from 3.28 to 3.45 Å (Table 1). In **(R_P,R_P)-[(+)$_{\delta}$-LNiBr]$_{2}$** the plane of the metal substituents P2−P1−P1′−Br is heavily deformed by 25.97°. This strong deformation, which is typical for all (R_P,R_P) isomers

Table 1. Roof-angles, M···M distances, square deformations, chelate angles, and helicity of the dinuclear complexes **(S_P,S_P)-** and **(R_P,R_P)-[(+)$_{\delta}$-LMHal]$_2$**

	(S_P,S_P)-[(+)$_{\delta}$-LPdCl]$_2$ 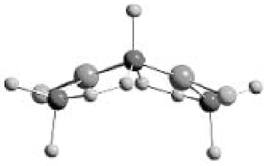		(R_P,R_P)-[(+)$_{\delta}$-LPdCl]$_2$ 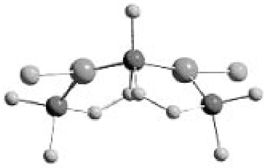
Complex	(S_P,S_P)	Data	(R_P,R_P)
[(+)$_{\delta}$-LNiBr]$_2$	140.84	roof angle [°] Ni−P1−P1′−Ni′	156.53
	3.277	distance [Å] Ni···Ni′	3.454
	7.71	square deformation [°] P2−P1−P1′−Br[a]	25.97
	10.5, δ	angle [°] Ni−P1−P2/C1−C2, helicity[b]	0.9, λ
[(+)$_{\delta}$-LPdCl]$_2$	141.31	roof angle [°] Pd−P1−P1′−Pd′	156.40
	3.422	distance [Å] Pd···Pd′	3.580
	7.33	square deformation [°] P2−P1−P1′−Cl[a]	22.92
	9.8, δ	angle [°] Pd−P1−P2/C1−C2, helicity[b]	2.6, λ
[(+)$_{\delta}$-LPdBr]$_2$	140.59	roof angle [°] Pd−P1−P1′−Pd′	
	3.419	distance [Å] Pd···Pd′	
	7.72	square deformation [°] P2−P1−P1′−Br[a]	
	10.7, δ	angle [°] Pd−P1−P2/C1−C2, helicity[b]	
[(+)$_{\delta}$-LPdI]$_2$	139.35	roof angle [°] Pd−P1−P1′−Pd′	
	3.410	distance [Å] Pd···Pd′	
	7.92	square deformation [°] P2−P1−P1′−I[a]	
	9.3, δ	angle [°] Pd−P1−P2/C1−C2, helicity[b]	
[(+)$_{\delta}$-LPtCl]$_2$	144.49	roof angle [°] Pt−P1−P1′−Pt′	
	3.477	distance [Å] Pt···Pt′	
	11.89	square deformation [°] P2−P1−P1′−Cl[a]	
	6.7, δ	angle [°] Pt−P1−P2/C1−C2, helicity[b]	

[a] Left square. [b] Chelate ring of left square.

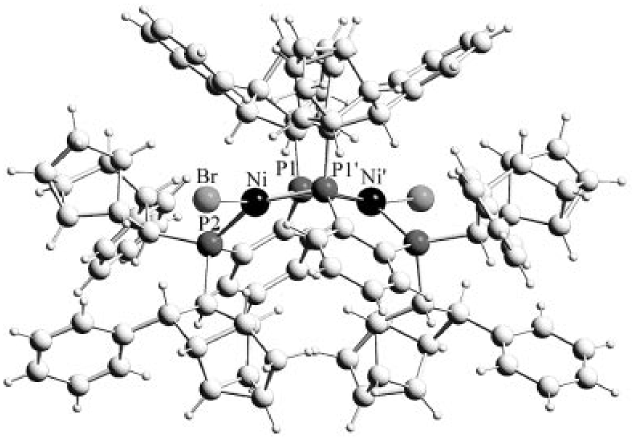

Figure 2. Molecular structure of **(R_P,R_P)-[(+)$_{\delta}$-LNiBr]$_2$**, crystallized from acetone; selected bond lengths [Å], bond angles [°], and dihedral angles [°]: Ni···Ni′ = 3.454(21), P1···P1′ = 2.650(11), Ni−Br = 2.344(4), Ni−P1 = 2.181(4), Ni−P1′ = 2.223(10), Ni−P2 = 2.201(4); Br−Ni−P1′ = 102.93(10), P1′−Ni−P1 = 73.96(1), P1−Ni−P2 = 90.19(2), P2−Ni−Br = 97.36(10), P1−Ni−Br = 168.28(11), P1′−Ni−P2 = 149.42(11); Ni−P1′−P1−Br = 7.43(7), Ni−P1′−P1−P2 = −18.54(9), P2−P1−P1′−Br = −25.97(10), Ni−P1−P1′−Ni′ = 156.53(15), Ni−P1−P2/C1−C2 = 0.9(6): λ

(Table 1), may be the reason for their discrimination compared to the (S_P,S_P) isomers. On the other hand, the chelate rings are almost planar in the (R_P,R_P) diastereomers. In **(R_P,R_P)-[(+)$_{\delta}$-LNiBr]$_2$** the inclination angle is only 0.9° with λ helicity (Table 1).

Similar to the NiBr series, it was possible in the PdCl series to isolate and characterize both diastereomers **(S_P,S_P)-** and **(R_P,R_P)-[(+)$_{\delta}$-LPdCl]$_2$** (Tables 1 and 3). The structural parameters (roof angle, nonbonding M−M distance, square deformation, inclination angle, and helicity) for the diastereomers **(S_P,S_P)-** and **(R_P,R_P)-[(+)$_{\delta}$-LPdCl]$_2$** link up with those of the diastereomers **(S_P,S_P)-** and **(R_P,R_P)-[(+)$_{\delta}$-LNiBr]$_2$**. Similar to the NiBr system, the two diastereomers of the PdCl system do not interconvert in solution, because their ^{31}P NMR spectra are different and stay different.

Using Na_2PdCl_4/LiBr, PdI_2, and **[(+)$_{\delta}$-LH)PtCl$_2$** as starting materials the dinuclear complexes **(S_P,S_P)-[(+)$_{\delta}$-LPdBr]$_2$**, **(S_P,S_P)-[(+)$_{\delta}$-LPdI]$_2$**, and **(S_P,S_P)-[(+)$_{\delta}$-LPtCl]$_2$** (Table 4) were isolated and characterized. They all belong to the (S_P,S_P) diastereomer series and resemble the (S_P,S_P) diastereomers described above in having roof angles about 140°, dihedral angels of the metal substituents between 7 and 12° and δ helicity in the slightly puckered chelate rings (Table 1).

The complex **(R_P)-[(+)$_\delta$-LPt$_2$Br$_3$(cod)]** was obtained during crystallization of **[(+)$_\delta$-LH)PtBr$_2$** which had been prepared from Pt(cod)Br$_2$ (Figure 3). The compound has only one **(+)$_\delta$-L$^-$** substituent which connects two platinum atoms by a single phosphido bridge. The configuration of this phosphorus atom was determined as (R_P). To one of the platinum atoms a cod molecule is coordinated, left over from the starting material Pt(cod)Br$_2$.

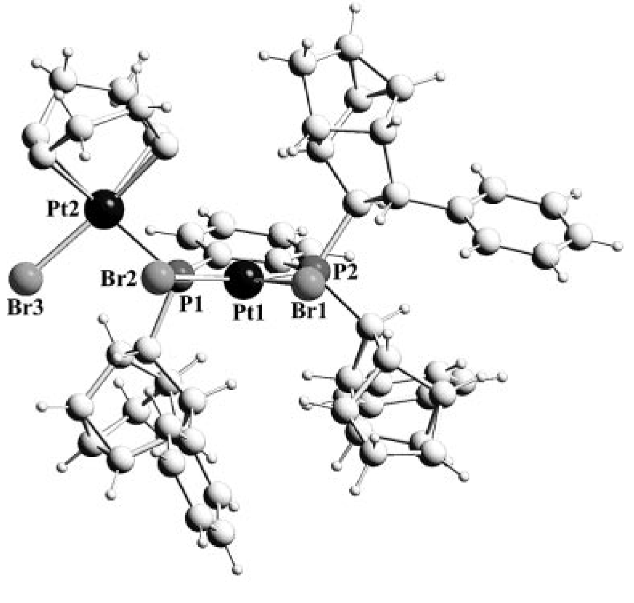

Figure 3. Molecular structure of **(R_P)-[(+)$_\delta$-LPt$_2$Br$_3$(cod)]**, crystallized from CH$_2$Cl$_2$/methanol; selected bond lengths [Å], bond angles [°], and dihedral angles [°]: Pt1···Pt2 = 3.832(2), Pt1−Br1 = 2.449(1), Pt1−Br2 = 2.507(1), Pt1−P1 = 2.249(2), Pt1−P2 = 2.239(2), Pt2−Br3 = 2.430(1), Pt2−P1 = 2.339(2); P1−Pt1−Br2 = 85.89(5), Br2−Pt1−Br1 = 88.98(3), Br1−Pt1−P2 = 97.11(5), P2−Pt1−P1 = 88.30(6), P1−Pt1−Br1 = 174.36(5), P2−Pt1−Br2 = 170.18(5), Pt1−P1−Pt2 = 113.27(7), P1−Pt2−Br3 = 94.98(4); Pt1−P1−Br2−P2 = 5.69(4), Pt1−P1−Br2−Br1 = −1.66(4), P1−Br2−Br1−P2 = 6.46(5), Pt1−P1−Br2−Pt2 = 140.28(7), Pt1−P1−Br2/Pt2−P1−Br3 = 78.18(8), Pt1−P1−P2/C1−C2 = 6.0(4): λ

The Unusual Trinuclear Phosphido-Bridged Complexes [(+)$_\delta$-L$_2$M$_3$Hal$_4$]

The dinuclear compounds **[(+)$_\delta$-LMHal]$_2$** discussed above are ubiquitous in the chemistry of palladium(II) and platinum(II). However, the trinuclear compounds **[(+)$_\delta$-L$_2$M$_3$Hal$_4$]** discussed here are extremely rare. Formally MX$_2$ is inserted into the dinuclear compounds **[(+)$_\delta$-LMHal]$_2$** as shown in Scheme 2.

Seven of the eight characterized trinuclear complexes were isolated during crystallization attempts of the mononuclear complexes **[(+)$_\delta$-LH]MHal$_2$**. Only the (R_P,R_P) isomer of the palladium chloride series was obtained by heating **(+)$_\delta$-LH** and PdCl$_2$ in toluene. As indicated in Scheme 2 (top) two mononuclear complexes in combination with MHal$_2$ give the trinuclear phosphido- and halide-bridged compounds by twofold HHal elimination.

Many isomers are possible for trinuclear compounds of the type **[(+)$_\delta$-L$_2$M$_3$Hal$_4$]**. All halogens can be oriented to one side and the two stereogenic phosphido phosphorus atoms may have the configurations (S_P,S_P), (R_P,R_P), and also (S_P,R_P). All three isomers have been isolated. In addi-

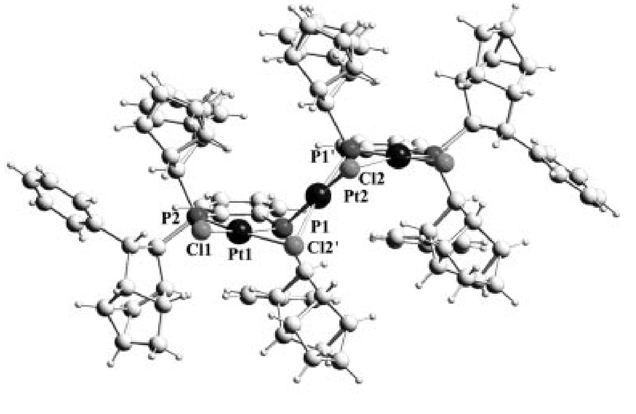

Figure 4. Molecular structure of **(S_P,S_P)-[(+)$_\delta$-L$_2$Pt$_3$Cl$_4$]** crystallized from CH$_2$Cl$_2$/methanol; selected bond lengths [Å] bond angles [°], and dihedral angles [°]: Pt1···Pt2 = 3.135(1), P1···Cl2 = 3.172(4), Pt1−P1 = 2.237(3), Pt1−Cl1 = 2.384(3), Pt1−Cl2 = 2.531(2), Pt1−P2 = 2.209(3), Pt2−P1 = 2.262(3), Pt2−Cl2 = 2.585(2); P2−Pt1−P1 = 88.54(10), P1−Pt1−Cl2 = 83.17(8), Cl2−Pt1−Cl1 = 88.37(8), Cl1−Pt1−P2 = 99.65(10), P2−Pt1−Cl2 = 171.49(8), P1−Pt1−Cl1 = 169.45(10), P1−Pt2−P1′ = 112.83(9), Cl2−Pt2−Cl2′ = 84.46(7), P1−Pt2−Cl2 = 81.47(8), P1−Pt2−Cl2′ = 165.51(8); Pt1−P1−Cl2−P2 = −1.40(6), Pt1−P1−Cl2−Cl1 = −4.38(7), P1−Cl2−Cl1−P2 = 2.62(9), Pt2−P1−Cl2−Cl2′ = 2.55(6), Pt2−P1−Cl2−P1′= −2.37(5), P1−P1′−Cl2′−Cl2 = 4.96(7), Pt1−P1−Cl2−Pt2 = 121.42(10), Pt1−P1−P2/C1−C2 = 4.0(6): δ

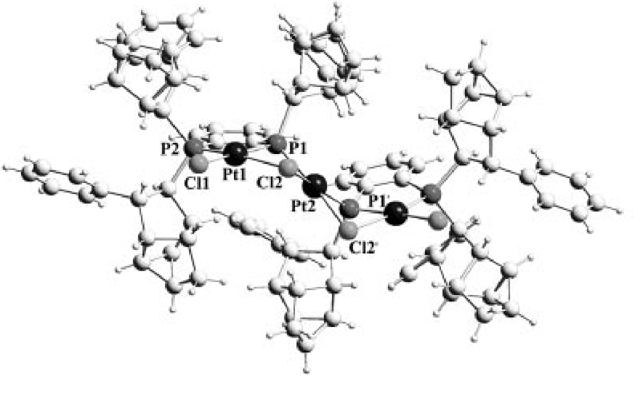

Figure 5. Molecular structure of **(R_P,R_P)-[(+)$_\delta$-L$_2$Pt$_3$Cl$_4$]**, crystallized from CH$_2$Cl$_2$/ethanol; selected bond lengths [Å], bond angles [°], and dihedral angles [°]: Pt1···Pt2 = 3.206(32), P1···Cl2 = 3.050(4), Pt1−P1 = 2.236(24), Pt1−Cl1 = 2.385(21), Pt1−Cl2 = 2.434(8), Pt1−P2 = 2.215(4), Pt2−P1 = 2.254(2), Pt2−Cl2 = 2.450(11); P2−Pt1−P1 = 88.61(7), P1−Pt1−Cl2 = 81.41(6), Cl2−Pt1−Cl1 = 89.29(7), Cl1−Pt1−P2 = 100.63(8), P2−Pt1−Cl2 = 169.54(7), Cl1−Pt1−P1 = 170.67(8), P1−Pt2−P1′ = 112.44(7), Cl2′−Pt2−Cl2 = 85.90(6), Cl2−Pt2−P1 = 80.71(6), P1−Pt2−Cl2′ = 165.95(6); Pt1−P1−Cl2−Cl1 = 0.55(5), Pt1−P1−Cl2−P2 = 2.27(5), P1−Cl2−Cl1−P2 = 1.50(7), Pt2−P1−Cl2−Cl2′ = −3.15(5), Pt2−P1−Cl2−P1′ = 1.37(4), P1−P1′−Cl2′−Cl2 = −4.50(6), Pt1−P1−Cl2−Pt2 = 128.96(7), Pt1−P1−P2/C1−C2 = 3.9(4): δ

Table 2. Roof angles, M···M distances, square deformations, chelate angles, and helicity of the trinuclear complexes **(S_P,S_P)-**, **(R_P,R_P)-**, and **(S_P,R_P)-[(+)$_\delta$-$L_2M_3Hal_4$]**

(S_P,S_P)-[(+)$_\delta$-$L_2Pd_3Br_4$]

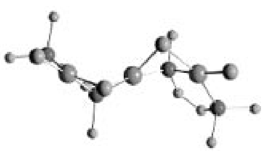

(R_P,R_P)-[(+)$_\delta$-$L_2Pd_3Br_4$]

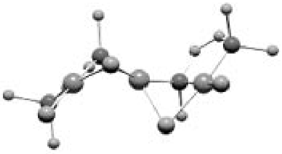

Complex	(S_P,S_P)	Data	(R_P,R_P)
[(+)$_\delta$-$L_2Pd_3Cl_4$]	132.02	roof angle [°] Pd1−P1−Cl2−Pd2	128.69
	3.223	distance [Å] Pd1···Pd2	3.157
	4.29, 0.68	square deformation [°][a]	6.02, 6.31
	5.8, δ	angle [°] Pd1−P1−P2/C1−C2, helicity[b]	1.83, δ
[(+)$_\delta$-$L_2Pd_3Br_4$]	124.02	roof angle [°] Pd1−P1−Br2−Pd2	156.40
	3.156	distance [Å] Pd1···Pd2	2.934
	12.41, 17.44	square deformation [°][a]	3.73, 29.29
	1.8, δ	angle [°] Pd1−P1−P2/C1−C2, helicity[b]	1.3, λ
[(+)$_\delta$-$L_2Pt_3Cl_4$]	121.42	roof angle [°] Pt1−P1−Cl2−Pt2	128.96
	3.135	distance [Å] Pt1···Pt2	3.206
	2.62, 4.96	square deformation [°][a]	1.50, 4.50
	4.0, δ	angle [°] Pt1−P1−P2/C1−C2, helicity[b]	3.9, δ
[(+)$_\delta$-$L_2Pt_3Br_4$]	127.16	roof angle [°] Pt1−P1−Br2−Pt2	132.77
	3.216	distance [Å] Pt1···Pt2	3.258
	12.47, 15.30	square deformation [°][a]	0.60, 12.09
	2.7, δ	angle [°] Pt1−P1−P2/C1−C2, helicity[b]	1.5, δ

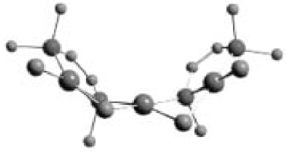

(S_P,R_P)-[(+)$_\delta$-$L_2Pt_3Br_4$]

[a] First entry left peripheral square P2−P1−Hal2−Hal1, second entry central square P1−P1′−Hal2′−Hal2. [b] Chelate ring of left peripheral square.

tion, there should be isomers having the halogens on different sides. Such isomers have not been observed up to now. The (+)-9-phenyldeltacyclanyl substituents in the trinuclear compounds have the same stereochemistry. It is the configuration of the two stereogenic phosphorus atoms which gives rise to the differences between the diastereomers.

The three isomers for the trinuclear complexes having all the halides on one side are shown at the bottom of Scheme 2. In the PdCl, PdBr, and PtCl series the diastereomers **(S_P,S_P)-** and **(R_P,R_P)-[(+)$_\delta$-$L_2M_3Hal_4$]** could be isolated and characterized. In the PtBr series the diastereomers **(S_P,S_P)-** and **(S_P,R_P)-[(+)$_\delta$-$L_2M_3Hal_4$]** were obtained.

All the new complexes are bent at the phosphido and halo bridges. This bending leads to chair and boat configurations for the three-square arrays in the trinuclear complexes **(S_P,S_P)-**, **(R_P,R_P)-**, and **(S_P,R_P)-[(+)$_\delta$-$L_2M_3Hal_4$]**. The chair configurations contain a C_2 axis passing through the central metal atoms. They subdivide into the diastereomers **(S_P,S_P)-** and **(R_P,R_P)-[(+)$_\delta$-$L_2M_3Hal_4$]** differing only in the phosphorus configuration. The isomer **(S_P,R_P)-[(+)$_\delta$-$L_2Pt_3Br_4$]** has a symmetry plane passing through the central Pt atom (without consideration of the chiral deltacyclanyl substituents). It is *meso*-configurated with respect to its central core.

Trinuclear compounds consisting of an array of three square-planar units connected by bridges are peculiar and rare. Whereas mononuclear compounds, such as $(PPh_3)_2PdCl_2$, and their chloro-bridged dinuclear pendants, e.g. $(PPh_3)ClPd(\mu\text{-}Cl)_2PdCl(PPh_3)$, are common, the corresponding trinuclear compound $(PPh_3)ClPd(\mu\text{-}Cl)_2Pd(\mu\text{-}Cl)_2PdCl(PPh_3)$ is unknown. For trinuclear phosphido-bridged complexes there is precedent in the literature.[11] In 2001 a series of new trinuclear complexes was described, which in contrast to our compounds (two phosphido and two halide bridges) contained four diphenylphosphido bridges.[12] An X-ray structural analysis of one of the trinuclear complexes showed a chair configuration with regard to the three-square array. The roof angles between the squares were 152.7° in agreement with our results.

The trinuclear compounds **(S_P,S_P)-** and **(R_P,R_P)-[(+)$_\delta$-$L_2Pt_3Cl_4$]** were isolated in attempts to crystallize **[(+)$_\delta$-LH)$PtCl_2$** from CH_2Cl_2 and CH_2Cl_2/EtOH, respectively. Both compounds were characterized by X-ray crystallography. A comparison of the structural parameters of the diastereomeric platinum chloride complexes **(S_P,S_P)-** and **(R_P,R_P)-[(+)$_\delta$-$L_2Pt_3Cl_4$]** shows that there are no large differences (Figures 4 and 5). The roof angles are very similar (121.42 and 128.96°, respectively) and the deformations of the peripheral and central squares P2−P1−Cl2−Cl1 and P1−P1′−Cl2′−Cl2 are insignificant (Table 2). The chelate rings Pt1−P1−C1−C2−P2 of the diastereomeric complexes are only slightly disturbed (2.7 and 1.5° respectively) both having δ chirality. Obviously, four chloride ligands on one side and four phosphorus atoms on the other side do not result in distinct distortions of the two diastereomers with opposite chair chirality.

With respect to structural aspects palladium compounds are similar to their platinum analogues. Accordingly, the palladium chloride diastereomers **(S_P,S_P)-** and **(R_P,R_P)-[(+)$_\delta$-$L_2Pd_3Cl_4$]** closely resemble their platinum congeners (Tables 2, 5 and 6).

In contrast to the platinum chloride and palladium chloride series, the two (S_P,S_P) and (R_P,R_P) diastereomers in the palladium bromide system show large differences (Tables 2 and 5). The roof angle of **(S_P,S_P)-[(+)$_\delta$-$L_2Pd_3Br_4$]** is more than 30° smaller than the roof angle of **(R_P,R_P)-[(+)$_\delta$-$L_2Pd_3Br_4$]**, which inversely affects the Pd−Pd distances. With 12.41 and 17.44°, respectively, the deformations of the peripheral and central squares P2−P1−Br2−Br1 and P1−P1′−Br2′−Br2 of the (S_P,S_P) diastereomer are strong but similar. In the (R_P,R_P) diastereomer, however, the peripheral squares are nearly undisturbed (3.73°), whilst the central square P1−P1′−Br2′−Br2 is extremely distorted (29.29°) as obvious from the formula in the upper right-hand corner of Table 2. The chelate rings in **(S_P,S_P)-** and **(R_P,R_P)-[(+)$_\delta$-$L_2Pd_3Br_4$]** are almost planar having opposite helicity (Table 2).

Similar to the trinuclear palladium bromide compounds the trinuclear platinum bromide complexes exhibited strong distortions. Table 2 shows that **(S_P,S_P)-[(+)$_\delta$-$L_2Pt_3Br_4$]** closely resembles the corresponding palladium derivative (Table 6) but the diastereomer **(R_P,R_P)-[(+)$_\delta$-$L_2Pt_3Br_4$]**, which would have been expected to be heavily distorted, could not be obtained at all. Instead, the only boat isomer **(S_P,R_P)-[(+)$_\delta$-$L_2Pt_3Br_4$]** was isolated (Figure 6, Table 2 bottom right).

In the boat isomer **(S_P,R_P)-[(+)$_\delta$-$L_2Pt_3Br_4$]** the left side (Table 2) and the right side of the molecule were appreciably different. Whereas the peripheral square on the right side was nearly planar (0.60°), the left and the central squares were distorted (13.90 and 11.97°, respectively). The boat isomer also had two unequal roof angles (left side 144.01°, right side 132.77°) resulting in a difference of the metal−metal distances of approximately 0.2 Å. The chelate rings Pt1−P1−C1−C2−P2 and Pt1′−P1′−C1′−C2′−P2′ on the two sides are only slightly disturbed (1.5 and 5.9°, respectively) both having δ chirality.

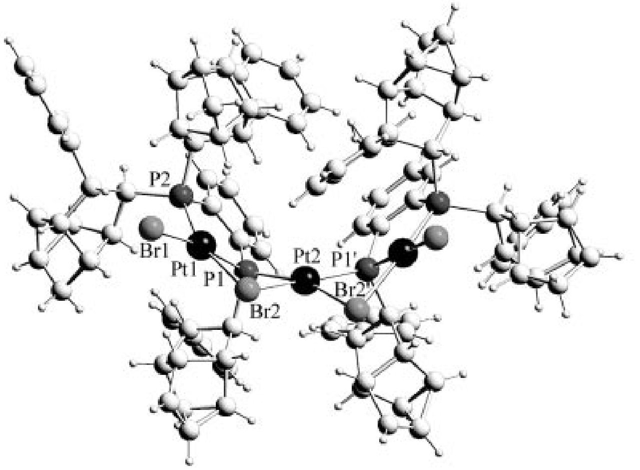

Figure 6. Molecular structure of **(R_P,S_P)-[(+)$_\delta$-$L_2Pt_3Br_4$]**, crystallized from benzene; selected bond lengths [Å], bond angles [°], and dihedral angles [°]: Pt1···Pt2 = 3.258(1), P1···Cl2 = 3.258(1), Pt1−P1 = 2.213(2), Pt1−Br1 = 2.483(2), Pt1−Br2 = 2.528(2), Pt1−P2 = 2.200(3), Pt2−P1 = 2.253(3), Pt2−Br2 = 2.575(2); P2−Pt1−P1 = 89.64(11), P1−Pt1−Br2 = 84.02(8), Br2−Pt1−Br1 = 89.82(5), Br1−Pt1−P2 = 96.41(9), P2−Pt1−Br2 = 173.37(9), P1−Pt1−Br1 = 173.19(9), P1−Pt2−Br2 = 82.15(8), P1−Pt2−P1′ = 113.87(11), Br2−Pt2−Br2′ = 84.68(5), P1−Pt2−Br2′ = 160.80(9); Pt1−P1−Br2−P2 = 1.37(6), Pt1−P1−Br2−Br1 = 2.05(6), P1−Br2−Br1−P2 = −0.60(8), Pt2−P1−Br2−Br2′ = −5.96(6), Pt2−P1−Br2−P1′ = 6.01(6), P1−P1′−Br2′−Br2 = −12.09(8), Pt1−P1−Br2−Pt2 = 132.77(11), Pt1−P1−P2/C1−C2 = 1.5(8): δ; Pt1′−P1′−P2′/C1′−C2′ = 5.9(7): δ

Experimental Section

General Remarks: All reactions were performed under dry nitrogen using standard Schlenk techniques. Solvents were purified and dried by standard procedures. *P,P,P′*-Tris[(+)-9-phenyldeltacyclan-8-yl)-1,2-bis(phosphanyl)benzene **[(+)$_\delta$-LH]** was prepared as described in the previous paper. Spectroscopy and analyses as in the previous paper. For the AA′XX′ systems in the ^{31}P NMR spectra the chemical shifts of the signals are given.

(S_P,S_P)-[(+)$_\delta$-LNiBr]$_2$: A suspension of **(+)$_\delta$-LH** (0.57 g, 0.77 mmol) and anhydrous $NiBr_2$ (0.18 g, 0.77 mmol) was heated for 30 min in ethanol (150 mL) in the presence of 2 g of Na_2CO_3. After cooling to room temperature, the red solution was concentrated, the residue dissolved in acetone and filtered through silica gel. Evaporation of the solvent and crystallization of the residue from CH_2Cl_2 provided **(S_P,S_P)-[(+)$_\delta$-LNiBr]$_2$** (0.20 g) as red crystals in 30% yield, m.p. > 250 °C. ^{1}H NMR ($CDCl_3$): δ = 3.48−0.38 (m, 60 H, aliph. H), 7.91−6.34 (m, 38 H, arom. H) ppm. ^{31}P NMR ($CDCl_3$): δ = 45.42, 44.99, 44.36, 43.93 (PR_2); −52.73, −53.17, −53.80, −54.23 (PR) ppm. MS (FD, CH_2Cl_2): *m/z* = 1724.6 [M$^+$].

(R_P,R_P)-[(+)$_\delta$-LNiBr]$_2$: A suspension of **(+)$_\delta$-LH** (0.32 g, 0.44 mmol) and anhydrous $NiBr_2$ (0.10 g, 0.44 mmol) was heated in CH_2Cl_2 (50 mL) for 1 h. After the addition of *n*BuLi (0.5 mL, 0.74 mmol, 1.6 M solution in hexane), the solution was heated for another 30 min, cooled to room temperature, filtered through silica gel, and concentrated. Crystallization from acetone provided **(R_P,R_P)-[(+)$_\delta$-LNiBr]$_2$** (0.20 g) as brown crystals in 54% yield, m.p. > 250 °C. ^{1}H NMR (CDCl$_3$): δ = 3.73−0.64 (m, 60 H, aliph. H), 7.90−5.90 (m, 38 H, arom. H) ppm. ^{31}P NMR (CDCl$_3$): δ = 44.78, 44.22, 43.68, 43.11, (PR$_2$); −69.86, −70.43, −70.98, −71.53 (PR) ppm. MS (FD, CH$_2$Cl$_2$): m/z = 1724.3 [M$^+$].

(S_P,S_P)-[(+)$_\delta$-LPdCl]$_2$: A suspension of **(+)$_\delta$-LH** (0.34 g, 0.47 mmol) and Na$_2$PdCl$_4$ (0.14 g, 0.47 mmol) in ethanol was stirred at room temperature for 36 h, followed by filtration through silica gel and concentration. Crystallization from CH$_2$Cl$_2$/Et$_2$O gave **(S_P,S_P)-[(+)$_\delta$-LPdCl]$_2$** (0.39 g) as pale yellow crystals in 95% yield, m.p. > 250 °C. C$_{102}$H$_{98}$Cl$_2$P$_4$Pd$_2$ (1731.5): calcd. C 70.75, H 5.70; found C 70.57, H 5.88. ^{1}H NMR (CDCl$_3$): δ = 4.95−0.20 (m, 60 H, aliph. H), 7.87−6.39 (m, 38 H, arom. H) ppm. ^{31}P NMR (CDCl$_3$): δ = 54.72, 54.00, 53.44, 51.96, 51.40, 50.71 (PR$_2$); −49.35, −50.07, −50.63, −52.11, −52.67, −53.37, (PR) ppm. MS (FAB, CH$_2$Cl$_2$): m/z = 1731.3 [M$^+$].

(R_P,R_P)-[(+)$_\delta$-LPdCl]$_2$: Compound **(+)$_\delta$-LH** (0.18 g, 0.25 mmol) and KO*t*Bu (0.028 g, 0.25 mmol) were stirred in THF. After 1 h, (PhCN)$_2$PdCl$_2$ (0.095 g, 0.25 mmol) was added to the pale yellow solution which was then stirred at room temperature for another 16 h. Evaporation of the solvent provided **(R_P,R_P)-[(+)$_\delta$-LPdCl]$_2$** (0.20 g) as a dark orange powder in 93% yield, m.p. > 250 °C. C$_{102}$H$_{98}$Cl$_2$P$_4$Pd$_2$ (1731.5): calcd. C 70.75, H 5.70; found C 70.52, H 5.93. ^{1}H NMR (CDCl$_3$): δ = 5.06−0.34 (m, 60 H, aliph. H), 7.94−6.28 (m, 38 H, arom. H) ppm. ^{31}P NMR (CDCl$_3$): δ = 60.73, 60.01, 56.31, 57.92, 57.22, 56.49 (PR$_2$); −72.25, −72.97, −73.66, −75.06, −75.75, −76.47, (PR) ppm. MS (FAB, CH$_2$Cl$_2$): m/z = 1731.3 [M$^+$].

(S_P,S_P)-[(+)$_\delta$-LPdBr]$_2$: Na$_2$PdCl$_4$ (0.094 g, 0.32 mmol) and a twelvefold excess of LiBr (0.34 g) were suspended at room temperature in 20 mL of ethanol. After 30 min, **(+)$_\delta$-LH** (0.23 g, 0.32 mmol) was added to the dark red solution, which was stirred for another 16 h. Filtration through silica gel and evaporation of the solvent gave **(S_P,S_P)-[(+)$_\delta$-LPdBr]$_2$** (0.27 g) as an orange powder in 94% yield, m.p. > 250 °C. C$_{102}$H$_{98}$Br$_2$P$_4$Pd$_2$ (1820.4): calcd. C 67.30, H 5.43; found C 67.05, H 5.59. ^{1}H NMR (CDCl$_3$): δ = 5.05−0.15 (m, 60 H, aliph. H), 7.86−6.36 (m, 38 H, arom. H) ppm. ^{31}P NMR (CDCl$_3$): δ = 55.11, 54.45, 53.90, 52.41, 51.86, 51.21 (PR$_2$); −51.73, −52.40, −52.95, −54.44, −54.99, −55.66 (PR) ppm. MS (ESI, CH$_3$OH): m/z = 1820.2 [M$^+$].

(S_P,S_P)-[(+)$_\delta$-LPdI]$_2$: Compound **(+)$_\delta$-LH** (0.24 g, 0.33 mmol) and PdI$_2$ (0.12 g, 0.33 mmol) were suspended in toluene and stirred at

Table 3. Crystal data, data collection, structure refinement, and CCDC numbers

	(S_P,S_P)-[(+)$_\delta$-LNiBr]$_2$	**(R_P,R_P)-[(+)$_\delta$-LNiBr]$_2$**	**(S_P,S_P)-[(+)$_\delta$-LPdCl]$_2$**	**(R_P,R_P)-[(+)$_\delta$-LPdCl]$_2$**
Empirical formula	$C_{102}H_{98}Br_2Ni_2P_4 \cdot 2CH_2Cl_2$	$C_{102}H_{98}Br_2Ni_2P_4$	$C_{102}H_{98}Cl_2P_4Pd_2$	$C_{102}H_{98}Cl_2P_4Pd_2 \cdot 1.5C_3H_6O$
M_r	1894.72	1724.87	1731.43	1818.50
Crystal system	monoclinic	triclinic	monoclinic	monoclinic
Space group	$P2_1$	$P1$	$P2_1$	$P2_1$
Z	2	1	2	2
Unit cell dimensions	a = 11.1744(7) Å b = 25.1435(11) Å c = 15.5240(9) Å β = 94.157(7) °	a = 10.3853(6) Å b = 14.1556(8) Å c = 16.8320(11) Å α = 107.957(7)° β = 95.405(7)° γ = 104.448(7)°	a = 11.2145(9) Å b = 25.2275(12) Å c = 15.6089(10) Å β = 93.020(8)°	a = 10.3483(7) Å b = 26.2025(12) Å c = 18.0479(12) Å β = 91.314(8)°
Volume	4350.2(4) Å^3	2239.8(3) Å^3	4409.8(5) Å^3	4892.4(5) Å^3
$D_{calcd.}$	1.446 g/cm^3	1.279 g/cm^3	1.304 g/cm^3	1.234 g/cm^3
Absorption coefficient	1.60 mm^{-1}	1.43 mm^{-1}	0.59 mm^{-1}	0.534 mm^{-1}
$F(000)$	1960	896	1792	1888
Crystal size	0.30 × 0.26 × 0.18 mm	0.24 × 0.16 × 0.04 mm	0.30 × 0.15 × 0.06 mm	0.40 × 0.30 × 0.25 mm
Crystal shape	prism	plate	plate	prism
Crystal color	red	brown	colorless	yellow
θ range for data collection	1.83−25.78°	2.22−25.17°	1.99−25.78°	1.92−25.19°
Limiting indices	$-13 \le h \le 13$ $-30 \le k \le 30$ $-18 \le l \le 18$	$-10 \le h \le 12$ $-15 \le k \le 16$ $-20 \le l \le 19$	$-13 \le h \le 13$ $-30 \le k \le 30$ $-28 \le l \le 18$	$-12 \le h \le 12$ $-31 \le k \le 31$ $-21 \le l \le 21$
Reflections collected	39823	12586	39695	52100
Independent reflections (R_{int})	16334 (0.0503)	11690 (0.0903)	16357 (0.0695)	17488 (0.0387)
Reflections $I > 2\sigma(I)$	14147	6183	13803	14440
Data/restraints/parameters	16334/1/1045	11690/3/991	16357/1/991	17488/1/1002
Absorption correction	numerical	numerical	none	none
Transmission (min/max)	0.8087/0.7268	0.9357/0.7861	−/−	−/−
Goodness-of-fit on F^2	1.412	0.807	0.983	0.966
Final R indices [$I > 2\sigma(I)$]	R_1 =0.0323 wR_2 = 0.0618	R_1 =0.0605 wR_2 = 0.1301	R_1 = 0.0458 wR_2 = 0.1035	R_1 = 0.0362 wR_2 = 0.0904
R indices (all data)	R_1 =0.0404 wR_2 = 0.0626	R_1 =0.1023 wR_2 = 0.1434	R_1 = 0.0534 wR_2 = 0.1062	R_1 = 0.0446 wR_2 = 0.0935
Absolute structure parameter	0.01(1)	0.02(1)	−0.03(2)	−0.01(1)
Largest diff. peak/hole	1.028/−0.383 e Å^{-3}	0.582/−0.656 e Å^{-3}	1.865/−0.627 e Å^{-3}	2.459/−0.474 e Å^{-3}
CCDC-	179308	179311	179309	179312

Table 4. Crystal data, data collection, structure refinement, and CCDC numbers

	$(S_\mathrm{P},S_\mathrm{P})$-[(+)$_\delta$-LPdBr]$_2$	**$(S_\mathrm{P},S_\mathrm{P})$-[(+)$_\delta$-LPdI]$_2$**	**(S_P,S_P)-[(+)$_\delta$-LPtCl]$_2$**	**(R_P)-[(+)$_\delta$-LPt$_2$Br$_3$(cod)]**
Empirical formula	$C_{102}H_{98}Br_2P_4Pd_2 \cdot 2CH_2Cl_2$	$C_{102}H_{98}I_2P_4Pd_2 \cdot 2CH_2Cl_2$	$C_{102}H_{98}Cl_2P_4Pt_2 \cdot CH_2Cl_2$	$C_{59}H_{57}Br_3P_2Pt_2 \cdot C_6H_6$
M_r	1990.18	2084.18	1993.68	1535.96
Crystal system	monoclinic	monoclinic	monoclinic	monoclinic
Space group	$P2_1$	$P2_1$	$P2_1$	$P2_1$
Z	2	2	2	4
Unit cell dimensions	a = 11.2099(7) Å b = 25.1732(11) Å c = 15.6498(10) Å β = 93.853(8)°	a = 11.2685(4) Å b = 25.1820(13) Å c = 15.6705(5) Å β = 93.332(4)°	a = 10.8345(5) Å b = 15.8537(8) Å c = 25.3733(15) Å β = 97.999(7)°	a = 23.3980(15) Å b = 10.6649(7) Å c = 24.8351(17) Å β = 109.9660(7)°
Volume	4406.2(4) Å^3	4439.2(3) Å^3	4315.9(4) Å^3	5824.8(7) Å^3
$D_{\mathrm{calcd.}}$	1.500 g/cm^3	1.559 g/cm^3	1.534 g/cm^3	1.752 g/cm^3
Absorption coefficient	1.56 mm^{-1}	1.34 mm^{-1}	3.485 mm^{-1}	6.950 mm^{-1}
F(000)	2032	2104	2004	2976
Crystal size	0.65 × 0.40 × 0.12 mm	0.12 × 0.08 × 0.04 mm	0.40 × 0.10 × 0.10 mm	0.32 × 0.20 × 0.08 mm
Crystal shape	prism	prism	prism	plate
Crystal color	yellow	yellow	colorless	colorless
θ range for data collection	2.08−25.81°	1.98−25.78°	2.07−25.89°	1.85−25.80°
Limiting indices	$-13 \le h \le 13$ $-30 \le k \le 30$ $-19 \le l \le 19$	$-13 \le h \le 10$ $-30 \le k \le 30$ $-18 \le l \le 17$	$-13 \le h \le 12$ $-19 \le k \le 19$ $-31 \le l \le 30$	$-28 \le h \le 28$ $-13 \le k \le 13$ $-30 \le l \le 30$
Reflections collected	62739	23846	32914	61516
Independent reflections (R_{int})	16897 (0.0390)	15618 (0.0619)	16160 (0.0558)	22238 (0.0521)
Reflections $I > 2\sigma(I)$	15985	9593	13960	16785
Data/restraints/parameters	16897/1/1045	15618/1/1045	16160/1/1018	22238/1/1297
Absorption correction	numerical	empirical	numerical	numerical
Transmission (min/max)	0.8416/0.5277	0.823/0.459	0.7326/0.5938	0.6144/0.2603
Goodness-of-fit on F^2	0.996	0.631	0.970	0.872
Final R indices [$I > 2\sigma(I)$]	R_1 = 0.0221 wR_2 = 0.0520	R_1 = 0.039 wR_2 0.0593	R_1 = 0.0379 wR_2 = 0.0880	R_1 = 0.0305 wR_2 = 0.0673
R indices (all data)	R_1 = 0.0241 wR_2 = 0.0526	R_1 = 0.0814 wR_2 = 0.0710	R_1 = 0.0444 wR_2 = 0.0896	R_1 = 0.0423 wR_2 = 0.0696
Absolute structure parameter	0.00(1)	−0.04(2)	−0.01(1)	−0.03(1)
Largest diff. peak/hole	0.644/−0.389 e Å^{-3}	0.593/−0.786 e Å^{-3}	2.618/−0.702 e Å^{-3}	2.649/−0.913 e Å^{-3}
CCDC-	179315	179316	179322	179319

room temperature for 16 h. Filtration through silica gel, evaporation of the solvent and crystallization from CH_2Cl_2/Et_2O provided **$(S_\mathrm{P},S_\mathrm{P})$-[(+)$_\delta$-LPdI]$_2$** (0.25 g) as red crystals in 78% yield, m.p. > 250 °C. $C_{102}H_{98}I_2P_4Pd_2$ (1914.4): calcd. C 63.90, H 5.30; found C 64.04, H 5.17. ^{1}H NMR ($CDCl_3$): δ = 5.25−0.14 (m, 60 H, aliph. H), 7.84−6.42 (m, 38 H, arom. H) ppm. ^{31}P NMR ($CDCl_3$): δ = 56.63, 56.01, 55.48, 53.99, 53.47, 52.84 (PR_2); −61.50, −62.12, −62.64, −64.14, −64.66, −65.29 (PR) ppm. MS (ESI, CH_2Cl_2): m/z = 1914.9 [M$^+$].

$(S_\mathrm{P},S_\mathrm{P})$-[(+)$_\delta$-LPtCl]$_2$: Compound **$(S_\mathrm{P},S_\mathrm{P})$-[(+)$_\delta$-LPtCl]$_2$** was isolated as colorless crystals during crystallization of **[(+)$_\delta$-LH]PtCl$_2$** (described in the previous paper) in CH_2Cl_2/MeOH, m.p. > 250 °C. ^{1}H NMR ($CDCl_3$): δ = 5.07−0.20 (m, 60 H, aliph. H), 7.83−6.38 (m, 38 H, arom. H) ppm. ^{31}P NMR ($CDCl_3$): δ = 49.94, 49.53, 49.23, 47.52, 47.23, 46.76 (PR_2); −67.53, −67.99, −68.26, −70.02, −70.30, −70.76 (PR, $^1J_{\mathrm{PtP}}$ = 2009 Hz) ppm. MS (ESI, CH_2Cl_2/MeOH): m/z = 1873.2 [(M − Cl)$^+$].

(R_P)-[(+)$_\delta$-LPt$_2$Br$_3$(cod)]: Compound **(R_P)-[(+)$_\delta$-LPt$_2$Br$_3$(cod)]** was isolated during crystallization of **[(+)$_\delta$-LH)PtBr$_2$** [described in the previous paper and prepared from Pt(cod)Br_2] in benzene.

$(S_\mathrm{P},S_\mathrm{P})$-[(+)$_\delta$-L$_2Pd_3Cl_4$]: Compound **$(S_\mathrm{P},S_\mathrm{P})$-[(+)$_\delta$-L$_2Pd_3Cl_4$]** was isolated as orange crystals during crystallization of **[(+)$_\delta$-LH]PdCl$_2$** (described in the previous paper) in CH_2Cl_2/Et_2O, m.p. > 250 °C. ^{1}H NMR ($CDCl_3$): δ = 4.93−0.23 (m, 60 H, aliph. H), 7.88−6.42 (m, 38 H, arom. H) ppm. ^{31}P NMR ($CDCl_3$): δ = 101.24, 101.21 (PR); 71.17, 71.14, 71.10, 71.06 (PR_2) ppm. MS (FAB, CH_2Cl_2): m/z = 1908.3 [M$^+$].

$(R_\mathrm{P},R_\mathrm{P})$-[(+)$_\delta$-L$_2Pd_3Cl_4$]: Compound **(+)$_\delta$-LH** (0.20 g, 0.28 mmol) and $PdCl_2$ (0.05 g, 0.28 mmol) were heated in toluene (50 mL) for 16 h. After cooling to room temperature, the dark red solution was filtered through silica gel and concentrated. Crystallization from CH_2Cl_2/Et_2O provided **$(R_\mathrm{P},R_\mathrm{P})$-[(+)$_\delta$-L$_2Pd_3Cl_4$]** (0.18 g) as orange crystals in 52% yield, m.p. > 250 °C. $C_{102}H_{98}Cl_4P_4Pd_3$ (1908.8): calcd. C 64.18, H 5.17; found C 64.05, H 5.30. ^{1}H NMR ($CDCl_3$): δ = 4.95−0.20 (m, 60 H, aliph. H), 7.89−6.39 (m, 38 H, arom. H) ppm. ^{31}P NMR ($CDCl_3$): δ = 95.71, 95.58, 95.56, 95.50, 95.47, 95.35 (PR); 74.01, 73.88, 73.85, 73.80, 73.77, 73.65 (PR_2) ppm. MS (FAB, CH_2Cl_2): m/z = 1908.5 [M$^+$].

$(S_\mathrm{P},S_\mathrm{P})$-[(+)$_\delta$-L$_2Pd_3Br_4$]: Compound **$(S_\mathrm{P},S_\mathrm{P})$-[(+)$_\delta$-L$_2Pd_3Br_4$]** was isolated as red crystals during crystallization of **[(+)$_\delta$-LH]PdBr$_2$** (described in the previous paper) in CH_2Cl_2/Et_2O, m.p. > 250 °C. $C_{102}H_{98}Br_4P_4Pd_3$ (2086.6): calcd. C 58.71, H 4.73; found C 58.22, H 5.10. ^{1}H NMR ($CDCl_3$): δ = 4.95−0.20 (m, 60 H, aliph. H), 7.89−6.39 (m, 38 H, arom. H) ppm. ^{31}P NMR ($CDCl_3$): δ =

Table 5. Crystal data, data collection, structure refinement, and CCDC numbers

	(S_P,S_P)-[(+)$_δ$-$L_2Pd_3Cl_4$]	**(R_P,R_P)-[(+)$_δ$-$L_2Pd_3Cl_4$]**	**(S_P,S_P)-[(+)$_δ$-$L_2Pd_3Br_4$]**	**(R_P,R_P)-[(+)$_δ$-$L_2Pd_3Br_4$]**
Empirical formula	$C_{102}H_{98}Cl_4P_4Pd_3$	$C_{102}H_{98}Cl_4P_4Pd_3 \cdot 3.25C_3H_6O$	$C_{102}H_{98}Br_4P_4Pd_3 \cdot 4C_6H_6 \cdot CH_2Cl_2$	$C_{102}H_{98}Br_4P_4Pd_3 \cdot 3C_4H_{10}O$
M_r	1908.68	2097.44	2483.91	2308.88
Crystal system	orthorhombic	orthorhombic	orthorhombic	orthorhombic
Space group	$P2_12_12$	$C222_1$	$P22_12_1$	$P2_12_12_1$
Z	4	4	2	4
Unit cell dimensions	a = 16.1149(15) Å b = 23.404(4) Å c = 26.315(3) Å	a = 15.1572(7) Å b = 19.8262(8) Å c = 37.3399(19) Å	a = 10.8826(4) Å b = 16.8315(10) Å c = 29.5292(12) Å	a = 10.5228(6) Å b = 29.3284(14) Å c = 32.6634(17) Å
Volume	9925(2) Å^3	11221.0(9) Å^3	5408.9(4) Å^3	10080.5(9) Å^3
$D_{calcd.}$	1.277 g/cm^3	1.242 g/cm^3	1.525 g/cm^3	1.472 g/cm^3
Absorption coefficient	0.752 mm^{-1}	0.674 mm^{-1}	2.130 mm^{-1}	2.23 mm^{-1}
F(000)	3904	4320	2516	4528
Crystal size	0.34 × 0.20 × 0.12 mm	0.40 × 0.24 × 0.20 mm	0.20 × 0.10 × 0.08 mm	0.26 × 0.10 × 0.03 mm
Crystal shape	plate	prism	prism	plate
Crystal color	red	red	orange	red
θ range for data collection	2.00−25.99°	2.01−25.14°	1.83−25.26°	1.87−24.78°
Limiting indices	$-19 \le h \le 18$ $-28 \le k \le 28$ $-32 \le l \le 30$	$-18 \le h \le 18$ $-23 \le k \le 23$ $-44 \le l \le 44$	$-12 \le h \le 12$ $-20 \le k \le 20$ $-35 \le l \le 34$	$-12 \le h \le 12$ $-34 \le k \le 34$ $-38 \le l \le 38$
Reflections collected	69751	35924	40151	69645
Independent reflections (R_{int})	18994 (0.1856)	9999 (0.0329)	9693 (0.0392)	17170 (0.1024)
Reflections $I > 2\sigma(I)$	13910	9690	8775	11165
Data/restraints/parameters	18994/0/497	9999/0/518	9693/0/632	17170/0/1058
Absorption correction	none	none	numerical	numerical
Transmission (min/max)	−/−	−/−	0.8008/0.7209	0.8816/0.6554
Goodness-of-fit on F^2	1.051	1.095	0.988	0.893
Final R indices [$I > 2\sigma(I)$]	R_1 = 0.1171 wR_2 = 0.2913	R_1 = 0.0278 wR_2 = 0.0831	R_1 = 0.0261 wR_2 = 0.0601	R_1 = 0.0567 wR_2 = 0.1029
R indices (all data)	R_1 = 0.1349 wR_2 = 0.3065	R_1 = 0.0294 wR_2 = 0.0837	R_1 = 0.0305 wR_2 = 0.0612	R_1 = 0.0964 wR_2 = 0.1135
Absolute structure parameter	0.18(6)	−0.02(2)	0.00(1)	0.02(1)
Largest diff. peak/hole	6.233/−1.097 e Å^{-3}	0.792/−0.675 e Å^{-3}	0.487/−0.650 e Å^{-3}	1.272/−0.639 e Å^{-3}
CCDC-	179313	179310	179317	179314

104.65, 104.60, 104.40, 104.29 (PR); 73.81, 73.75, 73.71, 73.66 (PR_2) ppm. MS (ESI, CH_3OH): m/z = 2086.2 [M^+].

(R_P,R_P)-[(+)$_δ$-$L_2Pd_3Br_4$]: Compound **(R_P,R_P)-[(+)$_δ$-$L_2Pd_3Br_4$]** was isolated as red crystals during crystallization of **[(+)$_δ$-LH]$PdBr_2$** (described in the previous paper) in acetone m.p. > 250 °C.

(S_P,S_P)-[(+)$_δ$-$L_2Pt_3Cl_4$]: Compound **(S_P,S_P)-[(+)$_δ$-$L_2Pt_3Cl_4$]** was isolated as yellow crystals during crystallization of **[(+)$_δ$-LH]$PtCl_2$** (described in the previous paper) in CH_2Cl_2.

(R_P,R_P)-[(+)$_δ$-$L_2Pt_3Cl_4$]: Compound **(R_P,R_P)-[(+)$_δ$-$L_2Pt_3Cl_4$]** was isolated as yellow crystals during crystallization of **[(+)$_δ$-LH]$PtCl_2$** (described in the previous paper) in CH_2Cl_2/ethanol, m.p. > 250 °C. $C_{102}H_{98}Cl_4P_4Pt_3$ (2174.8). ^1H NMR ($CDCl_3$): δ = 4.95−0.23 (m, 60 H, aliph. H), 7.86−6.16 (m, 38 H, arom. H) ppm. ^{31}P NMR ($CDCl_3$): δ = 43.81 (PR); 18.21 (PR_2) ppm. MS (ESI, CH_2Cl_2/CH_3OH): m/z = 2139.1 [(M − Cl)$^+$].

(S_P,S_P)-[(+)$_δ$-$L_2Pt_3Br_4$]: Compound **(S_P,S_P)-[(+)$_δ$-$L_2Pt_3Br_4$]** was isolated as yellow crystals during crystallization of **[(+)$_δ$-LH]$PtBr_2$** (described in the previous paper) in benzene and in CH_2Cl_2/EtOH, m.p. > 250 °C. $C_{102}H_{98}Br_3P_4Pt_3$ (2352.6): calcd. C 52.07, H 4.20, Br 13.59; found C 53.26, H 4.85, Br 13.12. ^1H NMR ($CDCl_3$): δ = 5.16−0.20 (m, 60 H, aliph. H), 7.66−6.09 (m, 38 H, arom. H) ppm. ^{31}P NMR ($CDCl_3$): δ = 49.32 (PR); 10.74 (PR_2, $^1J_{PtP}$ = 4374 Hz) ppm. MS (ESI, CH_2Cl_2/MeOH): m/z = 2272.6 [(M − Br)$^+$].

(R_P,S_P)-[(+)$_δ$-$L_2Pt_3Br_4$]: Compound **(R_P,S_P)-[(+)$_δ$-$L_2Pt_3Br_4$]** was isolated as yellow crystals during crystallization of **[(+)$_δ$-LH]$PtBr_2$** (described in the previous paper) in CH_2Cl_2/ethanol m.p. > 250 °C. MS (ESI CH_2Cl_2/MeOH): m/z = 2272.6 [(M − Br)$^+$].

X-ray Crystallographic Studies: The data were collected with a STOE-IPDS diffractometer with Mo-K_α radiation and graphite monochromator at a temperature of 173(1) K. Crystal data, data collection, structure refinement, and CCDC numbers for all complexes are given in Tables 3−6. The structures were solved by direct methods (SIR-97) and refined by full-matrix least squares on F^2 (SHELXL-97). The H atoms were calculated geometrically and a riding model was applied during the refinement process. Absorption corrections, when necessary, were carried out numerically from crystal shape (x-RED)[13] or emperical (PLATON)[14]. CCDC numbers given in Tables 3−6 contain the supplementary crystallographic data for this paper. These data can be obtained free of charge at www.ccdc.cam.ac.uk/conts/retrieving.html or from the Cambridge Crystallographic Data Centre 12 Union Road Cambridge CB2 1EZ, UK [Fax: (internat.) + 44-1223/336-033; E-mail: deposit@ccdc.cam.ac.uk].

Table 6. Crystal data, data collection, structure refinement, and CCDC numbers

	(S_P,S_P)-[$(+)_\delta$-$L_2Pt_3Cl_4$]	**(R_P,R_P)-[$(+)_\delta$-$L_2Pt_3Cl_4$]**	**(S_P,S_P)-[$(+)_\delta$-$L_2Pt_3Br_4$]**	**(S_P,R_P)-[$(+)_\delta$-$L_2Pt_3Br_4$]**
Empirical formula	$C_{102}H_{98}Cl_4P_4Pt_3\cdot CH_3OH$	$C_{102}H_{98}Cl_4P_4Pt_3\cdot CH_2Cl_2$	$C_{102}H_{98}Br_4P_4Pt_3\cdot 4C_6H_6$	$C_{102}H_{98}Br_4P_4Pt_3$
M_r	2206.77	2259.66	2662.95	2352.53
Crystal system	orthorhombic	monoclinic	orthorhombic	orthorhombic
Space group	$P222_12_1$	$P2_1$	$P222_12_1$	$P2_12_12_1$
Z	4	2	4	4
Unit cell dimensions	a = 16.6511(9) Å	a = 14.554(3) Å	a = 10.8380(4) Å	a = 10.6592(6) Å
	b = 21.5999(14) Å	b = 21.655(4) Å	b = 16.7888(7) Å	b = 25.4143(13) Å
	c = 26.1655(17) Å	c = 16.011(3) Å	c = 29.7005(15) Å	c = 37.398(2) Å
	β = 90°	β = 103.54(2)°	β = 90°	β = 90°
Volume	9410.7(10) Å^3	4905.9(17) Å^3	5404.2(4) Å^3	10131.0(9) Å^3
$D_{calcd.}$	1.558 g/cm^3	1.530 g/cm^3	1.637 g/cm^3	1.542 g/cm^3
Absorption coefficient	4.677 mm^{-1}	4.540 mm^{-1}	5.461 mm^{-1}	5.815 mm^{-1}
F(000)	4360	2228	2620	4576
Crystal size	0.26 × 0.16 × 0.06 mm	0.69 × 0.52 × 0.10 mm	0.52 × 0.20 × 0.12 mm	0.18 × 0.17 × 0.17 mm
Crystal shape	plate	plate	plate	prism
Crystal color	yellow	yellow	yellow	yellow
θ range for data collection	1.73−25.14°	1.95−25.07°	1.83−25.25°	1.69−23.85°
Limiting indices	$-19 \le h \le 19$	$-17 \le h \le 17$	$-12 \le h \le 12$	$-12 \le h \le 12$
	$-25 \le k \le 25$	$-25 \le k \le 25$	$-20 \le k \le 20$	$-28 \le k \le 28$
	$-31 \le l \le 31$	$-19 \le l \le 19$	$-35 \le l \le 35$	$-42 \le l \le 42$
Reflections collected	57178	63890	57351	66093
Independent reflections (R_{int})	16522 (0.0828)	17287 (0.0647)	9732 (0.0851)	14904 (0.0868)
Reflections $I > 2\sigma(I)$	12317	16162	8984	12959
Data/restraints/parameters	16522/0/1031	17287/1/1045	9732/0/558	14904/0/998
Absorption correction	numerical	numerical	numerical	numerical
Transmission (min/max)	0.7474/0.4094	0.6125/0.0900	0.6035/0.3017	0.5512/0.3228
Goodness-of-fit on F^2	0.926	1.034	1.026	1.036
Final R indices [$I > 2\sigma(I)$]	R_1 = 0.0427	R_1 = 0.0351	R_1 = 0.0298	R_1 = 0.0542
	wR_2 = 0.0923	wR_2 = 0.086	wR_2 = 0.0732	wR_2 = 0.1277
R indices (all data)	R_1 = 0.0657	R_1 = 0.0380	R_1 = 0.0334	R_1 = 0.0629
	wR_2 = 0.0978	wR_2 = 0.0875	wR_2 = 0.0747	wR_2 = 0.1314
Absolute structure parameter	−0.01(1)	0.01(1)	−0.03(1)	0.02(1)
Largest diff. peak/hole	2.670/−0.728 e Å^{-3}	1.646/−1.315 e Å^{-3}	1.489/−0.476 e Å^{-3}	2.964/−1.065 e Å^{-3}
CCDC-	179323	179321	179320	179318

---

[1] H. Brunner, S. Dormeier, M. Zabel, *Eur. J. Inorg. Chem.*, **2002**, 2594−2602.

[2] H. Brunner, M. Muschiol, F. Prester, *Angew. Chem.* **1990**, *102*, 680; *Angew. Chem. Int. Ed. Engl.* **1990**, *29*, 653.

[3] H. Brunner, F. Prester, *J. Organomet. Chem.* **1991**, *414*, 401.

[4] H. Brunner, A. Reimer, *Chem. Ber./Recueil* **1997**, *130*, 1495.

[5] S. Dormeier, Dissertation, Universität Regensburg, **2001**.

[6] G. Aullón, G. Ujaque, A. Lledós, S. Alvarez, P. Alemany, *Inorg. Chem.* **1998**, *37*, 804.

[7] G. Aullón, A. Lledós, S. Alvarez, *Inorg. Chem.* **2000**, *39*, 906.

[8] A. J. Carty, F. Hartstock, N. J. Taylor, *Inorg. Chem.* **1982**, *21*, 1349.

[9] T. Gebauer, G. Frenzen, K. Dehnicke, *Z. Naturforsch., Teil B* **1992**, *47*, 1505.

[10] M. A. Zhuravel, J. R. Moncarz, D. S. Glueck, *Organometallics* **2000**, *19*, 3447.

[11] R. Glaser, D. J. Kountz, R. D. Waid, J. C. Gallucci, D. W. Meek, *J. Am. Chem. Soc.* **1984**, *106*, 6324.

[12] E. Alonso, J. M. Casas, J. Forniés, C. Fortuno, A. Martin, A. G. Orpen, C. A. Tsipis, A. C. Tsipis, *Organometallics* **2001**, *20*, 5571.

[13] x-RED: Program for reduction of IPDS-data, version 1.10, STOE & Cie GmbH, Darmstadt, **1998**.

[14] A. L. Spek, *Acta Crystallogr., Sect. A* **1990**, *46*, C-34.

Received February 20, 2002
[I02097]